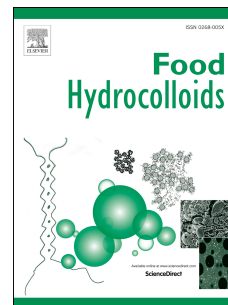


# Accepted Manuscript

Nanoparticles assembled from mixtures of whey protein isolate and soluble soybean polysaccharides. Structure, interfacial behavior and application on emulsions subjected to freeze-thawing

Darío M. Cabezas, Guido N. Pascual, Jorge R. Wagner, Gonzalo G. Palazolo



PII: S0268-005X(18)31788-0

DOI: <https://doi.org/10.1016/j.foodhyd.2019.04.040>

Reference: FOOHYD 5069

To appear in: *Food Hydrocolloids*

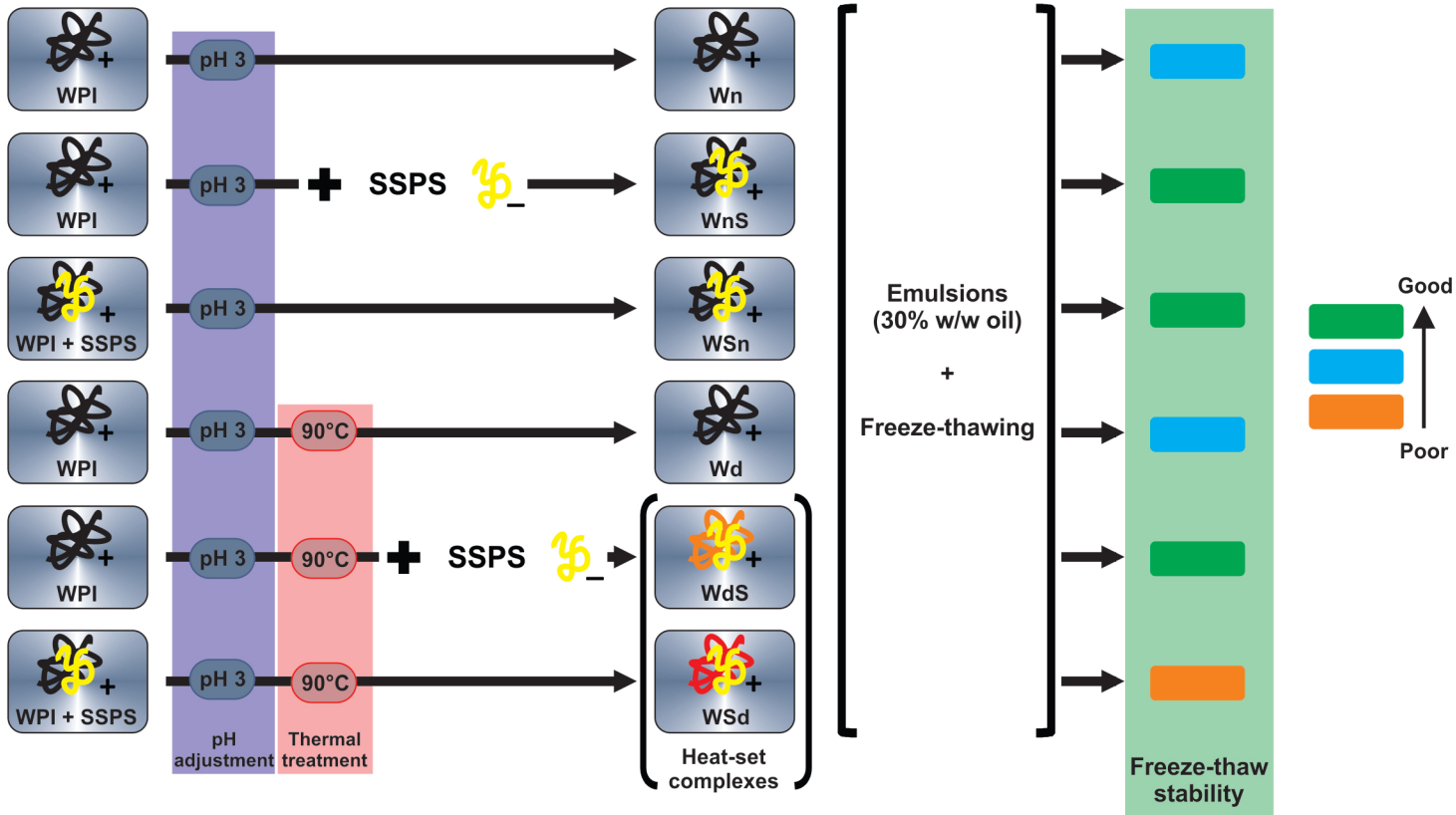
Received Date: 17 September 2018

Revised Date: 15 April 2019

Accepted Date: 18 April 2019

Please cite this article as: Cabezas, Darío.M., Pascual, G.N., Wagner, J.R., Palazolo, G.G., Nanoparticles assembled from mixtures of whey protein isolate and soluble soybean polysaccharides. Structure, interfacial behavior and application on emulsions subjected to freeze-thawing, *Food Hydrocolloids* (2019), doi: <https://doi.org/10.1016/j.foodhyd.2019.04.040>.

This is a PDF file of an unedited manuscript that has been accepted for publication. As a service to our customers we are providing this early version of the manuscript. The manuscript will undergo copyediting, typesetting, and review of the resulting proof before it is published in its final form. Please note that during the production process errors may be discovered which could affect the content, and all legal disclaimers that apply to the journal pertain.



1 **NANOPARTICLES ASSEMBLED FROM MIXTURES OF WHEY PROTEIN**  
2 **ISOLATE AND SOLUBLE SOYBEAN POLYSACCHARIDES. STRUCTURE,**  
3 **INTERFACIAL BEHAVIOR AND APPLICATION ON EMULSIONS SUBJECTED**  
4 **TO FREEZE-THAWING.**

5

6 Darío M. Cabezas<sup>a,b</sup>, Guido N. Pascual<sup>a</sup>, Jorge R. Wagner<sup>a,b</sup>, Gonzalo G. Palazolo<sup>a,b,\*</sup>

7

8 <sup>a</sup> Laboratorio de Investigación en Funcionalidad y Tecnología de Alimentos (LIFTA),  
9 Pabellón Dra. María C. Taira, Departamento de Ciencia y Tecnología, Universidad Nacional  
10 de Quilmes. Roque Sáenz Peña 352, Bernal, B1876BXD, Provincia de Buenos Aires,  
11 Argentina.

12 <sup>b</sup> Consejo Nacional de Investigaciones Científicas y Técnicas (CONICET), Godoy Cruz 2290,  
13 C1425FQB, Ciudad Autónoma de Buenos Aires, Argentina.

14

15 Darío M. Cabezas: [dario.cabezas@unq.edu.ar](mailto:dario.cabezas@unq.edu.ar)

16 Guido N. Pascual: [guidonpas@gmail.com](mailto:guidonpas@gmail.com)

17 Jorge R. Wagner: [jorge.wagner@unq.edu.ar](mailto:jorge.wagner@unq.edu.ar)

18 Gonzalo G. Palazolo (\*Corresponding author): [gonzalo.palazolo@unq.edu.ar](mailto:gonzalo.palazolo@unq.edu.ar)

19

20 Laboratorio de Investigación en Funcionalidad y Tecnología de Alimentos (LIFTA), Pabellón  
21 Dra. María C. Taira, Departamento de Ciencia y Tecnología, Universidad Nacional de  
22 Quilmes. Roque Sáenz Peña 352, Bernal, B1876BXD, Provincia de Buenos Aires, Argentina.

23 Tel: +54-11-43657100 ext. 5615, Fax: + 54-11-43657132

24

25  
26  
27  
28  
29  
30  
31  
32  
33  
34  
35  
36  
37  
38  
39  
40  
41  
42  
43  
44  
45  
46  
47  
48

## Abstract

In this article, the freeze-thaw stability of emulsions prepared with nanoparticles assembled from mixtures of whey protein isolate (WPI, 2.0% w/w) and soluble soybean polysaccharides (SSPS, 0.5% w/w) was assessed. The assembly was performed by pH adjustment to 3.0 without and with heating (90 °C, 15 min). Moreover, the order of addition of SSPS to proteins, before or after heating, was also studied. The complexes were characterized by dynamic light scattering, turbidity, non-sedimentable protein content, aromatic surface hydrophobicity ( $H_0$ ), interfacial tension and interfacial rheology measurements at the oil/water interface. In all cases, the dispersions evidenced slightly-positive  $\zeta$ -potential values due to electrostatic associative interactions between proteins and SSPS. Moreover, the complexation increased the particle size, the interfacial activity and the non-sedimentable protein content. Oil-in-water emulsions (30% w/w sunflower oil) prepared with unheated WPI/SSPS mixtures were more stable to freeze-thawing (-18 °C, 72 h; 20 °C, 2 h) respect to those prepared with WPI alone. When SSPS was added to previously heated proteins, the resultant emulsions also evidenced a high freeze-thaw stability. The large sedimentable species, which contributed to form a film of high viscoelasticity, could stabilize the emulsions by a Pickering mechanism. However, when SSPS and WPI were heated together, the resultant emulsions exhibited a low freeze-thaw stability due to a combination of poor emulsification ability and limited interfacial adsorption of large particles. The results of this article might have important implications in the preparation of highly acidic emulsion-based products resistant to freeze-thaw treatments.

49 **Keywords:** emulsions, freeze-thawing, nanoparticles, soluble soybean polysaccharides,  
50 stability, whey protein isolate.

51

## 52 **1. Introduction**

53

54 Freezing is a widely used technology that preserves the sensory and nutritional  
55 properties of foods, as well as the microbial and chemical spoilage (Thiebaud, Dumay, &  
56 Cheftel, 2002). Nevertheless, for emulsion-based products freeze-thaw treatments constitute  
57 an important environmental stress causing sometimes their breakdown, due to rupture of  
58 membranes surrounding the droplets. In oil-in-water emulsions, this allows oil-to oil contact,  
59 leading to extensive coalescence process and oiling off after thawing. Broadly, the freeze-  
60 thaw stability of emulsions depends on two main aspects: the crystallization of water and/or  
61 lipid phases and the drastic changes in microenvironmental conditions surrounding the  
62 droplets (pH, ionic strength, osmotic pressure and viscosity) (Degner, Chung, Schlegel,  
63 Hutkins, & McClements, 2014; Ghosh & Coupland, 2008). The improvement of freeze-thaw  
64 stability of oil-in-water emulsions was assessed through different approaches including the  
65 control of ice crystal growth, vitrification of continuous phase, addition of cryoprotectants and  
66 modification of interfacial structure (Degner et al., 2014; Ghosh, Cramp, & Coupland, 2006;  
67 Ghosh & Coupland, 2008; Palazolo, Sobral, & Wagner, 2016).

68 Interfacial engineering is one of most promising strategies for the stabilization of oil-  
69 in-water emulsions subjected to environmental stresses. The knowledge related with the  
70 interactions between proteins and polysaccharides is extremely important to assess the  
71 obtaining of emulsion-based foods resistant to freeze-thaw treatments. Indeed, the preparation  
72 of multilayered emulsions through layer-to-layer interfacial electrodeposition technique  
73 improved the stability freeze-thaw stability of emulsions, as was stated in previous papers

74 (Fioramonti, Arzeni, Pilosof, Rubiolo, & Santiago, 2015; Gu, Decker, & McClements, 2007).  
75 The improvement of stability was ascribed to the formation of a thick interfacial layer that  
76 resists the stress imposed by the expansion of ice during the freezing. Moreover, the papers  
77 concerning with the freeze-thaw stability of Pickering emulsions stabilized by food-grade  
78 particles is fast cumulating in recent years. Again, regardless the type of emulsifier, the  
79 formation of thick layer of aggregated particles at the oil/water interface contributes to the  
80 maintenance of stability after freeze-thawing. In this regard, Marefati, Rayner, Timgrem,  
81 Dejmek, & Sjö (2013) confirmed that the starch granule-base Pickering emulsions exhibited  
82 good freeze-thaw stability, which is enhanced by *in situ* partial gelatinization at the oil/water  
83 interface and the concomitant formation of gel-like network due to the presence of free starch  
84 particles in the aqueous phase. In other series of studies, the enhanced freeze-thaw stability of  
85 emulsions prepared with heated protein-based particles was attributed to the protein  
86 aggregation at the oil/water interface and the subsequent steric stabilization of droplets (Zhu,  
87 Zhang, Lin & Tang, 2017a; Zhu, Zheng, Liu, Qiu, Lin, & Tang, 2017b; Zhu, Zheng, Liu,  
88 Qiu, Lin, & Tang, 2018). This steric stabilization can be also achieved through the associative  
89 interactions between protein and polysaccharides at interfacial level, as was stated in a  
90 previous paper (Xu, Zhang, Cao, Wang, & Xiao, 2016).

91 On the other hand, milk proteins (caseins and whey proteins) are highly effective  
92 emulsifiers (Dickinson, 2016). Whey protein isolate (WPI) is an important by-product of the  
93 cheese industry and it is mainly composed by  $\beta$ -lactoglobulin,  $\alpha$ -lactalbumin,  
94 immunoglobulins, protease peptone, lactoferrin, glycomacropeptide and other minor proteins  
95 (Madureira, Pereira, Gomes, Pintado, & Malcata, 2007). WPI was widely used as the sole  
96 emulsifier or combined with polysaccharides in emulsion systems (Jiang et al., 2018;  
97 Laplante, Turgeon, & Paquin, 2005; Wang et al., 2017). In addition, whey protein-coated  
98 droplets are less prone to aggregation in highly-acid medium ( $\text{pH} < 4.0$ ) than soy protein

99 isolate or caseinate-coated droplets and may, therefore be more appropriate for use in acid  
100 emulsions (Degner et al., 2014).

101 Moreover, soluble soybean polysaccharides (SSPS) are a family of pectin-like acidic  
102 biopolymers used not only as a source of dietary fiber but also as a functional ingredient (Xu  
103 & Liu, 2016). This sample, extracted from soybean cotyledons, is composed mainly by of a  
104 main rhamnogalacturonan backbone branched by  $\beta$ -1,4-galactan and  $\alpha$ -1,3- or  
105  $\alpha$ -1,5-arabinan chains (Nakamura, Yoshida, Maeda, & Corredig, 2006). This polysaccharide  
106 sample can be classified as a surface-active polysaccharide. Nakamura, Yoshida, Maeda,  
107 Furuta, & Corredig (2004) separated the SSPS in two fractions by gel-filtration (310 kDa and  
108 20 kDa, respectively). The protein moieties associated to high-molecular weight fraction aid  
109 to adsorption of SSPS onto oil/water interface, explaining the good emulsifying properties of  
110 SSPS. SSPS have high water solubility, low bulk viscosity, low pH and high temperature  
111 stability (Xu & Liu, 2016). The interactions between proteins and SSPS in acid emulsions  
112 have been previously investigated. The presence of SSPS at high enough concentrations  
113 stabilized the sodium caseinate emulsions against acid-induced aggregation (Liu, Verespej,  
114 Alexander, & Corredig, 2007). In a relatively recent work, Ray & Rousseau (2013) reported  
115 that the complexes between SSPS and denatured soy-whey proteins improved the quiescent  
116 stability of emulsions in acidic medium. The stability would be ascribed to denser packing of  
117 complexes around the oil droplets, providing greater steric stabilization. Nevertheless, in the  
118 aforementioned studies, the freeze-thaw stability of the emulsions prepared with protein-  
119 SSPS complexes was not evaluated.

120 On the basis of above considerations, the aim of current work is to evaluate the impact  
121 of the complexation between whey proteins and SSPS on the freeze-thaw stabilization of acid  
122 o/w emulsions. The obtaining of nanoparticles assembled from mixtures of WPI and SSPS at  
123 pH 3.0 are proposed evaluating the impact of thermal treatments and the order of addition of

124 polysaccharides to protein in relation to the heating. The structural and interfacial behavior of  
125 nanoparticles at the oil/water interface was firstly evaluated; then, the freeze-thaw stability of  
126 oil-in-water emulsions prepared with the complexes was assessed.

127

## 128 **2. Materials and methods**

129

### 130 **2.1 Materials**

131

132 Whey protein isolate (WPI, Lacprodan<sup>®</sup> DI-9224) was donated by Arla Foods  
133 Ingredients Argentina, S.A (Martínez, Buenos Aires, Argentina). Its chemical composition (%  
134 w/w, as was given by the producer) was: crude protein (N×6.25), 86.5; lactose, 0.1; total fat,  
135 0.1 and salts, 1.25. Soluble soybean polysaccharides (SSPS, Soyafibe-S-CA100) were  
136 donated by Fuji Oil Co. Ltd (Osaka, Japan). Its chemical composition (% w/w, as given by the  
137 producer) was: total dietary fiber, 75.1; crude protein (N×6.25), 7.8; moisture, 5.8; crude  
138 ash, 7.8. Moreover, the SSPS saccharide composition (% w/w) was: rhamnose, 5.0; fucose,  
139 3.2; arabinose, 22.6; xylose, 3.7; galactose, 46.1; glucose, 1.2; galacturonic acid, 18.2. WSP  
140 and SSPS powder samples were used with no further purification. Refined sunflower oil was  
141 purchased in a local supermarket. 1-anilino-8-naphtalene sulfonate, ammonium salt (ANS)  
142 and  $\beta$ -lactoglobulin (> 90.0%, from bovine milk) were purchased from Sigma Co (MO,  
143 USA). All other chemical were analytical grade reagents purchased from Anedra (Research  
144 AG S.A; Buenos Aires, Argentina).

145

### 146 **2.2. Preparation of protein-polysaccharides dispersions**

147



148 Firstly, to ascertain the heating conditions to obtaining the nanoparticles, preliminary  
149 differential scanning calorimetry (DSC) assays were performed at pH 3.0 on concentrated  
150 WPI dispersions (20.0% w/w) in the absence and presence of SSPS (5.0% w/w). The pH  
151 adjustment was made by addition of 1.0 M HCl solution. Thermograms were obtained by  
152 heating samples at 5 °C/min from 20 to 120 °C (Q200 calorimeter, TA Instruments, Waters  
153 L.L.C; New Castle, DE USA), using an empty pan as reference. According to these assays, at  
154 pH 3.0, WPI dispersions showed only one endotherm (peak temperature,  $T_p = 79.38 \pm 0.05$   
155 °C; offset temperature,  $T_{\text{offset}} = 88.10 \pm 0.98$  °C; protein denaturation enthalpy,  $\Delta H = 5.87 \pm 0.83$   
156 J/g dry matter) which can be assigned to denaturation of  $\beta$ -lactoglobulin (Bernal & Jelen,  
157 1985). At the same pH, in the presence of SSPS,  $T_p$ ,  $T_{\text{offset}}$  and  $\Delta H$  were  $77.32 \pm 0.08$  °C,  
158  $86.10 \pm 0.50$  °C and  $\Delta H = 5.30 \pm 0.33$  J/g dry matter, respectively. On this basis, to perform the  
159 heating of dispersions, the temperature was set at 90 °C, where the WPI proteins were totally  
160 denatured.

161 The assembly of nanoparticles was performed by following the different strategies  
162 reported by Jones & McClements (2011) with some modifications: I) WPI and SSPS powders  
163 were jointly dispersed in distilled water by magnetic stirring for 2 h and the pH was adjusted  
164 to 3.0 by 1.0 M HCl addition. Aliquots of resultant dispersions (100 g) were heated at  $90.0 (\pm$   
165  $1.0)$  °C for 15 min with further cooling with running tap water to room temperature ( $25.0 \pm$   
166  $1.0$  °C); II) WPI powder was firstly dispersed in distilled water by magnetic stirring for 2 h  
167 and the pH was adjusted at 3.0 by 1.0 M HCl addition. The resultant dispersions (100 g) were  
168 heated at  $90.0 (\pm 1.0)$  °C for 15 min with further cooling with running tap water to room  
169 temperature ( $25.0 \pm 1.0$  °C). Then, SSPS powder was dispersed by magnetic stirring for 2 h,  
170 readjusting the pH to 3.0. In both cases, the final concentrations of WPI and SSPS were 2.0  
171 and 0.5% w/w, respectively (protein-to-polysaccharide mass ratio,  $R = 4.6$ ). Unheated  
172 WPI/SSPS dispersions and individual WPI and SSPS dispersions were used as control

173 samples. Heating of dispersions was performed in sealed tall-glass beakers (length: 60 mm;  
174 internal diameter, 25 mm). The temperature was monitored using a Lufft Opus C-10  
175 datalogger (Lufft, Meß und Regeltechnik, Germany); K thermocouples were located half way  
176 through dispersion. The warm up time was 5 min and the heating time (15 min) was  
177 registered once the dispersions reached the mentioned temperature at the center of the beaker.

178 Photographs at bulk scale of dispersions were performed using a digital camera  
179 (Kodak Easy Share, Eastman Kodak Company; Rochester, NY, USA). The nomenclature and  
180 visual appearance of all samples are summarized in Fig. 1.

181

### 182 ***2.3. pH dependence of turbidity of dispersions***

183

184 WPI, SSPS and WPI/SSPS ( $R= 4.6$ ) dispersions were prepared dispersing the powders  
185 with distilled water at 25 °C by mild magnetic stirring for 2 h to ensure total dispersion and  
186 hydration. The final concentrations of WPI and SSPS were 2.0 and 0.5% w/w, respectively.  
187 To perform acid titration assays, the dispersions were previously diluted with distilled water  
188 (1:3 v/v). The pH values of WPI, SSPS and WPI/SSPS diluted dispersions were  $6.90 \pm 0.02$ ,  
189  $5.95 \pm 0.01$  and  $6.62 \pm 0.02$ , respectively. Then, aliquots of these dispersions (20 ml) were  
190 titrated with repeated additions of 0.1 M HCl under mild magnetic stirring. The pH value was  
191 registered and the turbidity was expressed as the apparent optical density at 600 nm using a  
192 T60 UV-visible spectrophotometer (PG Instruments; Leicestershire, United Kingdom)

193

### 194 ***2.4. Determination of non-sedimentable protein content***

195

196 The determination of non-sedimentable protein content, which is a measure of the  
197 amount of protein incorporated into relatively small particles that cannot be removed by  
198 centrifugation at high speed, was determined by following the procedure reported by Jones &  
199 McClements (2010) with some modifications. Dispersions were placed in 50-ml screw-  
200 capped tubes and subsequently centrifuged at 19,000×g for 30 min at 20 °C (Sigma 3-18KS  
201 centrifuge, Sigma Laborzentrifugen GmbH; Osterode am Harz, Germany). Then, supernatants  
202 were carefully separated in glass tubes. Appropriate dilutions with 2.0 % w/v Na<sub>2</sub>CO<sub>3</sub>  
203 solution were made; then, the protein content was determined by the modified Lowry method  
204 (Markwell, Hass, Bieber, & Tolbert, 1978), using β-lactoglobulin as standard protein. The  
205 protein content was also measured on initial dispersions, without centrifugation. Thus, the  
206 non-sedimentable protein (% w/w) was calculated as:

$$\text{Non-sedimentable protein (\% w/w)} = (\text{sP/iP}) \times 100 \quad (1)$$

207  
208  
209  
210 sP is the protein content in the supernatant and iP is the protein content in the initial  
211 dispersion, without centrifugation.

### 212 213 **2.5. Particle size, ζ-potential and turbidity of nanoparticles**

214  
215 The hydrodynamic diameter (or z-average diameter, D<sub>Z</sub>) and ζ-potential of particles in  
216 different dispersions were determined at 25 °C by dynamic light scattering (DLS) using a  
217 Horiba Scientific nanoparticle analyzer SZ-100 (Horiba Ltd.; Kyoto, Japan). All the  
218 dispersions were diluted with double-distilled water, previously adjusted at pH 3.0 with HCl  
219 1.0 M, to avoid multiple light scattering effects. The D<sub>Z</sub> and ζ-potential were reported as the  
220 mean and standard deviation of two separate assays, with ten readings made per assay.

221 Moreover, the intra-particle interactive forces of particles in dispersions were  
222 evaluated by dissociation tests according to the method reported by Zhu et al. (2017a), with  
223 some modifications. The dispersions were diluted with distilled water (1:3 v/v) adjusted at pH  
224 3.0 with 1.0 M HCl in the absence and presence of 6.0 M urea, dithiothreitol (DTT, 30 mM),  
225 or their combinations. The final concentrations of urea and DTT in the diluted dispersions  
226 were 4.5 M and 22.5 mM, respectively. After being stored for 30 min, the turbidity of the  
227 diluted dispersions, expressed as the apparent optical density at 600 nm, was read using a T60  
228 UV-visible spectrophotometer (PG Instruments; Leicestershire, United Kingdom).

229

### 230 ***2.6. Aromatic surface hydrophobicity***

231

232 Aromatic surface hydrophobicity ( $H_0$ ) was determined by fluorescence using the ANS  
233 probe, according to method of Mitidieri & Wagner (2002) with some modifications.  
234 Dispersions were serially diluted with double-distilled water previously adjusted to pH 3.0  
235 with HCl solution to obtain protein concentrations ranging from  $1.0 \cdot 10^{-2}$  to  $1.0 \cdot 10^{-4}$  % w/v.  
236 Then, 40  $\mu$ l of ANS (8.0 mM in double-distilled water) was added to 3.0 ml of dispersions.  
237 Fluorescence intensity was measured at 365 nm (excitation wavelength) and 484 nm  
238 (emission wavelength) using a Scinco FluoroMate FS-2 fluorescence spectrometer (Scinco  
239 Co, Ltd, Seoul, Korea) ( $I_{F, ANS}$ ). Moreover, fluorescence intensity was measured in the same  
240 dispersions without ANS addition ( $I_F$ ). From the plot of  $\Delta I_F$  ( $I_{F, ANS} - I_F$ ) as a function of  
241 protein concentration,  $H_0$  was obtained as the initial slope. Finally,  $H_0$  was expressed as a  
242 relative value, taking that of  $W_n$  sample as reference ( $H_0 = 100$ ).

243

### 244 ***2.7. Interfacial behavior of nanoparticles***

245

246 The interfacial behavior of particles was evaluated through both the interfacial tension  
247 and interfacial rheology measurements at the oil/water interface. Both assays were carried out  
248 on dispersions (2.0% w/w WPI; 0.5% w/w SSPS) without previous dilution. The equilibrium  
249 interfacial tension was measured at 25 °C using an automated Lauda TD3 LMT 850  
250 tensiometer (Lauda Königshofen, Germany) associated to a Peltier thermostating unit. The Du  
251 Noüy ring measurement method was selected in the device. The interfacial tension values of  
252 double-distilled water (adjusted to pH 3.0 with HCl 1.0 M) and aqueous dispersions at the  
253 same pH ( $\gamma_{i, w}$  and  $\gamma_{i, d}$ , respectively) were obtained. Then, the equilibrium interfacial pressure  
254 ( $\pi_i$ ) was calculated as:

$$\pi_i = \gamma_{i, w} - \gamma_{i, d} \quad (2)$$

255  
256  
257  
258 In addition, the rheological properties of layers at oil/water interface were evaluated  
259 by the use of an oscillatory rheometer TA AR-G2 (TA Instruments, Waters, L.L.C;  
260 Newcastle, DE, USA) associated to a Du Noüy ring. Oscillatory shear measurements were  
261 performed at 25 °C, and at constant frequency of 0.1 Hz. The strain was set to 5.0% within the  
262 lineal viscoelastic range. The complex viscosity ( $\eta^*$ ) of layer, which includes both the elastic  
263 and the viscous responses, was calculated as:

$$\eta^* = [(G')^2 + (G'')^2]^{0.5} / \omega \quad (3)$$

264  
265  
266  
267  $G'$  is the interfacial elastic module,  $G''$  the interfacial viscous module and  $\omega$  the angular  
268 frequency. The overall evolvement of adsorption layer was monitored through the variation of  
269  $\eta^*$  as a function of time (Baldusdottir, Fullerton, Nielsen, & Jorgensen, 2010).

270

## 271 **2.8. Preparation of o/w emulsions**

272

273 A two-step homogenization process was used to prepare the emulsions. Firstly,  
274 aqueous dispersions (2.0% w/w WPI; 0.5% w/w SSPS) were mixed with refined sunflower oil  
275 (30% w/w) using a high-speed rotor/stator device (Ultraturrax T-25 homogenizer, S25N-8G  
276 dispersing tool at 25,000 rpm for 2 min, IKA Labortechnik; Staufen, Germany). Then, the  
277 pre-emulsions were poured in a beaker and sonicated in an ultrasound homogenizer (Sonics  
278 Vibra Cell VCX750, Sonics & Materials, Inc.; Newtown, CT, USA) at 70% amplitude, with  
279 the standard tip immersed 1/3 in a glass beaker (28 mm diameter) for 2 min. The temperature  
280 increase during sonication was avoided putting the beaker in a water-ice bath.

281

## 282 **2.9. Freeze-thaw protocol**

283

284 Emulsion samples were transferred to vertical plastic containers (internal diameter =  
285 30 mm with plastic lids), and the temperature was set at  $20.0 \pm 1.0$  °C. Then, they were  
286 isothermally stored in still air for 72 h at  $-18.0 \pm 2.0$  °C. After storage at subzero temperature,  
287 frozen samples were thawed into a water bath at  $20.0 \pm 1.0$  °C for 2 h, and kept at this  
288 temperature before further characterization analyses.

289

## 290 **2.10. Characterization of initial and freeze-thawed emulsions**

291

292 The particle size distribution(PSD) was obtained by laser diffraction using a Malvern  
293 Mastersizer 2000E analyzer associated to a Hydro 2000MU wet dispersion unit (Malvern  
294 Instruments Ltd.; Worcestershire, United Kingdom). Emulsions were previously diluted with  
295 distilled water or 1.0% w/v sodium dodecyl sulfate solution adjusted at pH 3.0. Then,

296 emulsions were poured into the dispersion unit and stirred continuously (2,000 rpm) to ensure  
297 the sample homogeneity during PSD measurements. The optical parameters used to obtain the  
298 PSD were: refractive index of dispersant, 1.33, refractive and adsorption indices for the  
299 particles, 1.47 and 0.01, respectively. Particle size results were expressed as De Brouckere,  
300 volume-weighted mean diameters ( $D_{4,3}$ ) and 90<sup>th</sup> percentile values ( $D_{v,0.9}$ ), which are more  
301 sensitive to the presence of large particles.

302 The flocculation index (FI, %) of initial or freeze-thawed emulsions, was calculated  
303 as:

$$304 \quad \text{FI \%} = [(D_{4,3} - D_{4,3 \text{ SDS}})/D_{4,3 \text{ SDS}}] \times 100 \quad (4)$$

305  
306  $D_{4,3}$  and  $D_{4,3 \text{ SDS}}$  are the De Brouckere mean diameters obtained from PSD measured in the  
307 absence and presence of SDS, respectively. This method allows evaluating only the flocs  
308 stable in the measurement conditions (Palazolo et al., 2011).

309 Moreover, the coalescence index (CI, %) of freeze-thawed emulsions was calculated  
310 as:

$$311 \quad \text{CI \%} = [(D_{4,3 \text{ f-t}} - D_{4,3 \text{ u}})/D_{4,3 \text{ u}}] \times 100 \quad (5)$$

312  
313  $D_{4,3 \text{ u}}$  and  $D_{4,3 \text{ f-t}}$  are the De Brouckere mean diameters obtained from PSD of initial and freeze-  
314 thawed emulsions, respectively. PSD were measured in the presence of SDS (Palazolo et al.,  
315 2011).

## 317 **2.11. Statistical analysis**

318  
319 All the characterization assays were conducted at least in triplicate and the results  
320 were expressed as mean  $\pm$  standard deviation. The statistical analysis was performed by

321 analysis of variance (ANOVA) and Fisher test using the statistical program Statgraphics  
322 Centurion 18<sup>®</sup> (Statgraphics Technologies Inc., The Plains, VA, USA, 2017). Significance  
323 was considered at  $p < 0.05$ .

324

### 325 **3. Results and discussion**

326

#### 327 *3.1. pH dependence of aqueous dispersions of whey protein isolate and soluble soybean* 328 *polysaccharides*

329

330 In this section, the pH-dependence of the turbidity of unheated and diluted (1:3 v/v)  
331 aqueous dispersions containing WPI, SSPS and WPI/SSPS mixture was studied. The results  
332 are shown in Fig. 2a. WPI dispersions were clear in the pH range from 6.0 to 7.0 and at pH  
333 lower than 3.5. Nevertheless, the turbidity abruptly increased when pH was in the range 3.5-  
334 5.5 (maximum at pH ~ 4.4), indicating that the protein self-association had occurred due to  
335 weakening to electrostatic repulsion between protein molecules, as was well-established in the  
336 literature. (Alting et al., 2003; Bryant & McClements, 1999). Conversely, the turbidity of  
337 SSPS dispersions was close to zero across the entire pH range (pH 7.0 to 2.0). Although it is  
338 known that a protein fraction is associated to polysaccharides in SSPS (Nakamura et al., 2004,  
339 2006), the electrostatic and steric repulsion between the negatively charged and branched  
340 polysaccharides molecules avoided their self-association.

341 On the other hand, the pH dependence of the turbidity of WPI/SSPS mixture was  
342 considerably different from that of the WPI and SSPS dispersions (Fig 2a, b). In the pH range  
343 from 6.0 to 7.0, the turbidity of WPI/SSPS mixture was only slightly higher respect to that of  
344 individual WPI dispersion. These results would be consistent with a low degree of interaction  
345 between protein and polysaccharides in the pH range 6.0-7.0, presumably because both the



346 protein and polysaccharide molecules have a relatively high net negative charge (Kobori et  
347 al., 2009). Indeed, according to Ibanoglu (2005), for proteins and carboxylated  
348 polysaccharides, the complexation becomes very weak at neutral pH. However, the turbidity  
349 increased with decreasing pH at pH below 5.3, had a maximum at pH ~ 4.3 and then slowly  
350 decreased until pH 2.0. Even though the protein-to-polysaccharide mass ratio was relatively  
351 high ( $R = 4.6$ ), the maximum value of turbidity of WPI noticeably decreased (~1.2 to ~0.6)  
352 and it was shifted to lower pH values in the presence of SSPS. The WPI content of all  
353 dispersions was the same, so that the presence of polysaccharides inhibited the ability of  
354 protein molecules to interact with each other and form large aggregates.  
355 These observations indicate the occurrence of interactions between the protein and  
356 polysaccharides present in the dispersions. Interestingly, the turbidity of WPI/SSPS mixture  
357 was fairly high in the range of pH from 2.5 to 3.5 (Fig 2a,b). Under these pH conditions the  
358 WPI and SSPS dispersions were completely clear (Fig 2b), so that the associative interactions  
359 between protein and polysaccharides in the mixture are still relatively strong. Thus, the  
360 assembly and characterization of nanoparticles was performed at pH 3.0.

361

### 362 ***3.2. Structural characterization of nanoparticles***

363

364  $W_n$  and  $W_d$  dispersions exhibited a clear appearance (Fig. 1) and their  $\zeta$ -potential were  
365 close to + 20 mV, which are in agreement with those reported by other authors (Benichou,  
366 Aserin, Lutz, & Garti, 2007) (Fig 3a). For SSPS clear dispersion (Fig. 1), the  $\zeta$ -potential was  
367 slightly negative; the magnitude of charge is low because the galacturonic acid has a  $pK_a$  near  
368 to 3.0. Consequently, the opposite net charges of polysaccharides and proteins favored the  
369 formation of complexes. Indeed, all mixed dispersions exhibited a turbid appearance,  
370 regardless the preparation method, and their  $\zeta$ -potential values were slightly positive (Figs. 1

371 and 3a). According to Benichou et al. (2007), WPI protein particles in the dispersions have a  
372 net charge equal to zero at pH 4.8. At pH 3.0, below the isoelectric point of the WPI, the  
373 numerous cationic groups on the protein molecules are partially neutralized by the anionic  
374 groups of SSPS, decreasing the  $\zeta$ -potential of complexes (Fig 3a). At the same pH, the  
375 decrease of  $\zeta$ -potential of soy proteins by SSPS complexation was also reported in previous  
376 papers (Ray & Rousseau, 2016; Xu & Liu, 2016).

377 Moreover, for all dispersions, the content of non-sedimentable protein (% w/w) is  
378 shown in Fig. 3b. This parameter was near to 100% for clear  $W_n$ ,  $W_d$  and SSPS dispersions  
379 and a slight, but significant decrease, was evidenced when both WPI and SSPS were mixed  
380 without any thermal treatment ( $WS_n$  and  $W_nS$ ), ( $p < 0.05$ ). In contrast, when heating was  
381 performed on dispersions, an additional reduction of non-sedimentable protein content was  
382 evidenced for  $WS_d$ . The positive net charge of all complexes was quite similar (Fig 3a) so that  
383 the particular behavior of  $WS_d$  complex can be influenced by other factors, such as the surface  
384 hydrophobicity and particle size. Indeed, the z-average values ( $D_z$ ) for species in the total and  
385 non-sedimentable fraction were also determined (Fig 3c). For the total fraction, all complexes  
386 exhibited larger particle sizes than those of  $W_n$ ,  $W_d$  and SSPS, regardless the thermal treatment  
387 ( $p < 0.05$ ). In turn,  $WS_d$  and  $W_dS$  complexes evidenced larger particle size respect to those  
388 assembled from unheated proteins ( $WS_n$  and  $W_nS$ ,  $p < 0.05$ ). In addition, the  $D_z$  values  
389 measured on the supernatants were lower respect to those of the total fraction for all  
390 complexes (Fig 3c,  $p < 0.05$ ), which would reflect that the relatively large particles were  
391 removed by centrifugation. The  $D_z$  values of  $WS_n$  and  $W_nS$  did not show significant  
392 differences ( $p > 0.05$ ). Conversely, noticeable differences were observed between the particle  
393 size of  $WS_d$  and  $W_dS$  complexes in the non-sedimentable fraction ( $p < 0.05$ ). These  
394 observations would support a different molecular organization of protein and polysaccharides  
395 for the complexes assembled in the heated dispersions.

396 In fact, the aromatic surface hydrophobicity ( $H_0$ ) was also determined (Fig 4a). As  
397 expected, SSPS evidenced very low  $H_0$  due to the presence of sugar polar groups, which  
398 impair the interaction of the fluorescent probe with the non-polar aminoacid residues of the  
399 SSPS protein fraction. The increase of  $H_0$  of  $W_n$  upon heating was consistent with the  
400 exposure of non-polar amino acids of WPI proteins, as was also previously reported (Zhu et  
401 al., 2017a). Nevertheless, for  $W_d$ , the increase of the intensity of hydrophobic interactions was  
402 not sufficient to promote the protein self-association due to electrostatic repulsion between  
403 protein molecules (Fig. 3a,b). With regard to the  $WS_n$  and  $W_nS$  complexes, the addition of  
404 SSPS to the proteins, slightly increased the  $H_0$  ( $p<0.05$ ). In both cases, the complexation  
405 between both biopolymers would promote an exposure of non-polar amino acid residues,  
406 though to a limited extent. The impact of SSPS addition on  $H_0$  was substantially different  
407 when the assembly was performed with denatured proteins. For  $W_dS$  complex, the significant  
408 decrease of  $H_0$  with respect to that of  $W_d$  ( $p<0.05$ ) would indicate that a shell of  
409 polysaccharides might be formed on the protein particles. This mechanism was also reported  
410 by Xu & Liu (2016) for nanoparticles assembled with soy protein isolates and SSPS. In  
411 contrast, when WPI and SSPS were heated together, an enhancing of  $H_0$  was effectively  
412 observed ( $p<0.05$ ). In this case, the globular proteins tend to stay associated with SSPS for a  
413 longer time during the thermal treatment (Jones & McClements, 2011). The increase of  $H_0$   
414 would be consistent with a higher degree of exposure of non-polar amino acid residues,  
415 indicating that the structural organization of protein and polysaccharides within the  $WS_d$   
416 complex might be different respect to that of  $W_dS$  one.

417 In this context, the internal structure of complexes was also investigated by monitoring  
418 the turbidity of the total fraction at pH 3.0 in the absence and presence of protein-perturbing  
419 agents, such as urea and DTT (Fig 5b). Overall, in the absence of urea and DTT, all systems  
420 evidenced higher turbidity values for  $WS_n$  and  $WS_d$  dispersions and they were not

421 significantly affected by the DTT addition (data not shown). In the presence of urea, the  
422 turbidity values of  $W_nS$  and  $WS_n$  were negligible whatever the DTT addition. In contrast, the  
423 turbidity of  $WS_d$  dispersion was fairly higher, showing a slight, but significant decrease with  
424 DTT addition ( $p < 0.05$ , Fig 5b). On the basis of these results, it can be hypothesized that  
425 hydrophobic effect as well as hydrogen and disulfide bonds would be also involved in the  
426 formation of nanoparticles, as was also stated in other systems (Liu & Xu, 2016, Zhu et al,  
427 2017a). The urea directly interacts with proteins via strong Van der Waals dispersive  
428 interactions with protein side-chains and backbone compared to water, which promotes the  
429 intrusion of urea molecules in the hydrophobic core and to urea's preferential binding to all  
430 regions of proteins (Hua, Zhou, Thirumalai & Berne, 2008; Kamerzell, Esfandiary, Joshi,  
431 Middaugh, & Volkin, 2011). This interaction weakens the hydrophobic core and disrupts the  
432 intramolecular hydrogen bonds. The  $\zeta$ -potential of  $W_dS$  and  $WS_d$  was similar ( $p > 0.05$ );  
433 however, for the latter complex, significantly higher values of non-sedimentable protein  
434 content, particle size and  $H_0$  were observed ( $p < 0.05$ , Figs 3b,c and 4a). Thus, the tighter  
435 interactions between protein and polysaccharides within the nanoparticles would increase  
436 their resistance to the perturbing effect of urea. Moreover, for  $WS_d$  complex, the formation of  
437 disulfide bonds via thiol-disulfide exchange would be promoted in a higher extent, although  
438 the extension of this reaction is limited in acidic medium (Monagan, Sherman, & Kinsella,  
439 1995). This latter observation was consistent with the slight decrease of turbidity by DTT  
440 addition in the presence of urea (Fig 4b).

441

### 442 ***3.3. Interfacial behavior of nanoparticles***

443

444 Firstly, the evolvement of the complex viscosity ( $\eta^*$ ) as a function of time is depicted  
445 in Fig. 5. For  $W_n$  and  $W_d$ , a steep increase of  $\eta^*$  was observed from the start of measurement

446 indicating a fast adsorption of protein molecules onto the oil/water interface (Baldursdottir et  
447 al, 2010, Fig 5a). Although  $W_d$  exhibited a high  $H_0$ , (Fig 4a) its interfacial pressure ( $\pi_i$ ) was  
448 slight, but significantly lower than that of  $W_n$  (Table 1,  $p < 0.05$ ). The protein adsorption is a  
449 complex process, and depends on various factors such as hydrophobicity, net charge, charge  
450 distribution, structure and molecular weight (Haynes & Norde, 1994). In this context, the  
451 denatured protein particles, which have a higher particle size (Fig 3c), would be less prone to  
452 efficiently accommodate at the oil/water interface, promoting a lower increase of  $\pi_i$ .  
453 Nevertheless, the higher intensity of attractive interactions forces between denatured particles  
454 already adsorbed to the interface was consistent with the formation of a film of a higher  
455 viscoelasticity (Fig 5a,b). On the other hand, with the exception of  $WS_d$ , the time dependency  
456 of  $\eta^*$  for all the other complexes was substantially different to that of  $W_n$  and  $W_d$  dispersions;  
457 the complex viscosity progressively increased with increasing time and it leveled off after 30  
458 min of adsorption, reaching higher  $\eta^*$  values at the end of assay (Fig 5a, b). At the same time,  
459  $WS_n$  and  $W_nS$  complexes evidenced a higher interfacial activity, showing a slight, but  
460 significant higher  $\pi_i$  values than those of  $W_n$ . In analyzing comparatively the  $\pi_i$  of  $WS_d$  and  
461  $W_dS$  complexes respect to that of  $W_d$  alone, a similar tendency was observed (Table 1,  $p <$   
462  $0.05$ ). The weakening of the electrostatic repulsion of protein molecules due to the  
463 complexation with SSPS (Fig 3a) would favor a more efficient adsorption at the oil/water  
464 interface of the complexes.

465 In order to elucidate if the large sedimentable particles can adsorb at the interface, the  
466 interfacial rheology tests were also performed on the non-sedimentable fraction (Fig 5c). For  
467 all complexes, a plateau at low  $\eta^*$  was reached from the start of measurement indicating a fast  
468 adsorption. Thus, the comparative analysis of the rheology profiles the total and non-  
469 sedimentable fractions revealed that the large sedimentable species play an important role in  
470 the stabilization of the interfacial film. These species slow down the adsorption rate, but at the

471 same time promote the formation of more viscoelastic films. This would be especially valid  
472 for  $WS_n$ ,  $WS_d$  and  $W_dS$  dispersions. Conversely, for  $WS_d$ , although the species present in non-  
473 sedimentable fraction evidenced a fast adsorption, the large particles would only have a  
474 limited ability to adsorb at the oil/water interface.

475

#### 476 **3.4. Characterization of initial and freeze-thawed emulsions**

477

478 The  $D_{4,3}$  and  $D_{v,0.9}$  values, obtained from PSD in the presence of SDS are shown in Fig  
479 6.  $WS_n$  and  $W_nS$  complexes evidenced a better emulsifying behavior respect to that of  $W_n$   
480 alone. According to Jafari, Assadpoor, He, & Bhandari (2008), the particle size of emulsions  
481 is the result of an equilibrium between droplet break-up and re-coalescence. In all cases, the  
482 concentration of emulsifier was high, so that there is enough emulsifier to cover the interface.  
483 Thus, the improved emulsifying behavior of  $WS_n$  and  $W_nS$  could be explained by a decrease  
484 of electrostatic repulsion, a concomitant increase of  $H_0$ ,  $\pi_i$ . (Figs. 3a and 4a; Table 1) and the  
485 ability of larger particles to reduce the re-coalescence during the emulsification. Conversely,  
486 for emulsions prepared with heated dispersions,  $D_{4,3}$  decreased in the order:  $WS_d > W_d > W_dS$   
487 ( $p < 0.05$ ) and  $WS_d$  exhibited the highest  $D_{v,0.9}$  value ( $p < 0.05$ , Fig 6 a,b). As was seen above,  
488 the large sedimentable particles of  $WS_d$  are poorly adsorbed (Fig 5b,c). Unlike the interfacial  
489 tension and interfacial rheology assays, during the ultrasound emulsification, the emulsifier  
490 adsorption is forced because the interfacial area is quickly created by cavitation (Jafari et al.,  
491 2008). In this condition, it is probable that the large sedimentable particles are also poorly  
492 adsorbed favoring the droplet re-coalescence and the resultant increase of particle size of  $WS_d$   
493 emulsion (Fig. 6).

494 Moreover, the flocculation index (FI) of all initial emulsions was quite similar and  
495 lower than 5% (Table 2). For emulsions prepared with protein as emulsifiers, only the flocs

496 formed by a bridging mechanism are stable in the measurement conditions of PSD (high  
497 dilution and stirring) (Gu et al., 2007). The bridging flocculation is especially promoted when  
498 there is not enough emulsifier to cover the interface (Palazolo et al., 2011). Thus, the low FI  
499 values obtained in all cases are supported by the high concentration of emulsifier in the  
500 emulsions.

501 It is known that the freeze-thawing is a highly destabilizing treatment for emulsions,  
502 (Ghosh et al., 2006, Palazolo et al., 2011, 2016, Thiebaud et al., 2002). After freeze-thawing,  
503 all emulsions were destabilized by coalescence and flocculation, though to a different extent  
504 (Table 2). It is worth noting that the emulsions were stored at subzero temperature during a  
505 relatively short time period and a low-melting-point oil phase was used. Hence, the mentioned  
506 differences could be mainly attributed to the processes that occur in the aqueous phase at  
507 interfacial level (Palazolo et al., 2011). Emulsions prepared with  $W_d$  dispersion showed  
508 slightly higher destabilization parameters (FI and CI, %) respect to that of  $W_n$  one ( $p < 0.05$ ).  
509 This result was similar respect to that obtained by Zhu et al (2017a) for emulsions prepared  
510 with unheated and heated WPI after one cycle of freeze-thawing. For  $W_nS$ ,  $W_dS$  and  $WS_n$   
511 emulsions, an improvement of stability to coalescence and flocculation upon freeze-thawing  
512 was effectively observed, showing CI and FI values lower than 17 and 20%, respectively.  
513 Conversely,  $WS_d$  emulsion exhibited the highest destabilization degree to coalescence and  
514 flocculation; the CI and FI values were higher than those of  $W_d$  emulsions, without SSPS  
515 addition (Table 2).

516 According to the Zhu et al (2017 a,b), the freeze-thaw stability of emulsions prepared  
517 with proteins as the sole emulsifier can be enhanced by a Pickering mechanism, due to the  
518 adsorption to protein aggregates onto the oil/water interface. In this paper, the role of large  
519 sedimentable particles could be critical to improve the freeze-thaw stability of the emulsions.  
520 The Pickering steric stabilization would be supported by the low magnitude of surface charge

521 of complexes (Fig 3a). The species present in the sedimentable fraction, which contribute  
522 with the formation of interfacial film of high viscoelasticity (Fig. 5b,c), could also adsorb  
523 during the emulsification, improving the freeze-thaw stability of the  $WS_n$ ,  $W_nS$  and  $W_dS$   
524 emulsions respect to those prepared with  $W_n$  and  $W_d$  alone. In contrast, for  $WS_d$  emulsions, the  
525 limited adsorption of large particles could have a negative impact on their freeze-thaw  
526 stability. Thus, the improvement of stability of  $WS_n$ ,  $W_nS$  and  $W_dS$  emulsions to freeze-  
527 thawing would be directly associated to a combination of enhanced emulsification ability of  
528 complexes and their structures at the oil/water interface.

529

#### 530 4. Conclusions

531

532 The present study has demonstrated that the improvement of the freeze-thaw stability  
533 of acid emulsions prepared with complexes assembled from whey protein isolate and soluble  
534 soybean polysaccharides would be ascribed to the adsorption of large particles during the  
535 emulsification, in agreement with the formation of an interfacial film of high viscoelasticity.  
536 The steric Pickering stabilization would be supported by the low net charge of complexes at  
537 pH 3.0. The behavior was clearly evident for the complexes obtained by assembly of unheated  
538 proteins and by the addition of polysaccharides to previously heated whey proteins.  
539 Conversely, the nanoparticles obtained when both biopolymers were heated together  
540 evidenced a low stability to freeze-thawing due to a limited adsorption of large particles at the  
541 oil/water interface. The internal organization of both biopolymers within the complexes,  
542 which was evidenced by measurements of surface hydrophobicity and turbidity in the  
543 presence of protein-perturbing agents, would play a key role to explain the differences in the  
544 adsorption behavior of both complexes obtained from heated dispersions. Although the  
545 complexation between protein and polysaccharides is a valid strategy to improve the stability



546 of emulsions against environmental stresses, such as the freeze-thawing, the impact of the  
547 assembly procedure of the nanoparticles cannot be dismissed. The results of this article might  
548 have important implications in the preparation of highly acidic emulsion-based products (such  
549 as sauces and beverages) resistant to environmental stresses, such as the freeze-thaw  
550 treatments.

551

## 552 **Acknowledgements**

553

554 The authors wish to thank Fuji Oil Co. Ltd (Osaka, Japan) for the provision of soluble  
555 soybean polysaccharides.

556

## 557 **Funding**

558

559 The authors greatly appreciate the financial support of Universidad Nacional de  
560 Quilmes (53/1037 I+D grant) and Agencia Nacional de Promoción Científica y Tecnológica  
561 (FONCyT, PICT 2014-1267 and PICT 2015-0084).

562

## 563 **References**

564

- 565 Alting, A.C., Hamerm R.J., de Kruif, C.G., de Jongh, H.H.J., Simons, J.F.A. & Visschers,  
566 R.W. (2003). Physical and chemical interactions in pH-induced aggregation and gelation of  
567 whey proteins. In: E. Dickinson, & T. Van Vliet (Eds). *Food Colloids, Biopolymers and*  
568 *Materials* (pp 49-58). Cambridge, UK: The Royal Society of Chemistry.
- 569 Baldursdottir, S.G.; Fullerton, M.S.; Nielsen, S.H. & Jorgensen, L. (2010). Adsorption of  
570 proteins at the oil/water interface. Observation of protein adsorption by interfacial shear

- 571 stress measurements. *Colloids and Surfaces B: Biointerfaces*, 79, 41-46.  
572 <https://doi.org/10.1016/j.colsurfb.2010.03.020>.
- 573 Benichou, A., Aserin, A., Lutz, R., & Garti, N. (2007). Formation and characterization of  
574 amphiphilic conjugates of whey protein isolate (WPI)/xanthan to improve surface activity.  
575 *Food Hydrocolloids*, 21, 379-391. <https://doi.org/10.1016/j.foodhyd.2006.04.013>.
- 576 Bernal, V. & Jelen, P. (1985). Thermal stability of whey proteins. A calorimetric study. *Journal*  
577 *of Dairy Science*, 68, 2847-2852. [https://doi.org/10.3168/jds.S0022-0302\(85\)81177-2](https://doi.org/10.3168/jds.S0022-0302(85)81177-2)
- 578 Bryant, C.M., & McClements, D.J. (1999). Ultrasonic spectrometry study of the influence of  
579 temperature on whey protein aggregation. *Food Hydrocolloids*, 13, 439-444.  
580 [https://doi.org/10.1016/S0268-005X\(99\)00018-1](https://doi.org/10.1016/S0268-005X(99)00018-1).
- 581 Degner, B.M., Chung, C., Schlegel, V., Hutkins, R., & McClements, D.J. (2014). Factors  
582 influencing the freeze-thaw stability of emulsion-based foods. *Comprehensive Reviews in*  
583 *Food Science and Food Safety*, 13, 98-113. <https://doi.org/10.1111/1541-4337.12050>.
- 584 Dickinson, E. (2016). Interfacial structure and stability of food emulsions as affected by  
585 protein-polysaccharide interactions. *Soft Matter*, 4, 932-942. doi: 10.1039/B718319D.
- 586 Fioramonti, S.A., Arzeni, C., Pisolof, A.M.R., Rubiolo, A.C. & Santiago, L.G. (2015).  
587 Influence of freezing temperature and maltodextrin concentration on stability of linseed  
588 oil-in-water multilayer emulsions. *Journal of Food Engineering*, 156, 31-38.  
589 <https://doi.org/10.1016/j.jfoodeng.2015.01.013>.
- 590 Ghosh, S., Cramp, G.L., & Coupland, J.N. (2006). Effect of aqueous composition on the  
591 freeze-thaw stability of emulsions. *Colloids and Surfaces A: Physicochemical and*  
592 *Engineering Aspects*, 272, 86-88. <https://doi.org/10.1016/j.colsurfa.2005.07.013>.
- 593 Ghosh S., & Coupland, J.N. (2008). Factors affecting the freeze-thaw stability of emulsions.  
594 *Food Hydrocolloids*, 22, 105-111. <https://doi.org/10.1016/j.foodhyd.2007.04.013>.

- 595 Gu, Y.S., Decker, E.A., & McClements, D.J. (2007). Application of multi-component  
596 biopolymer layers to improve the freeze-thaw stability of oil-in-water emulsions:  $\beta$ -  
597 lactoglobulin,  $\iota$ -carragenan-gelatin. *Journal of Food Engineering*, 80, 1246-1254.  
598 <https://doi.org/10.1016/j.jfoodeng.2006.09.015>.
- 599 Haynes, C.A., & Norde, W. (1994). Globular proteins at solid/liquid interfaces. *Colloids and*  
600 *Surfaces B. Biointerfaces*, 2, 517-566. [https://doi.org/10.1016/0927-7765\(94\)80066-9](https://doi.org/10.1016/0927-7765(94)80066-9).
- 601 Hua, L., Zhou, R., Thirumalai, D., & Berne, B.J. (2008). Urea denaturation by stronger  
602 dispersion interactions with proteins than water implies a 2-stage unfolding. *Proceedings*  
603 *of the National Academy of Sciences of the USA*, 105, 16928–16933.  
604 <https://doi.org/10.1073/pnas.0808427105>.
- 605 Ibanoglu, E. (2005). Effect of hydrocolloids on thermal denaturation of proteins. *Food*  
606 *Chemistry*, 90, 621-626. <https://doi.org/10.1016/j.foodchem.2004.04.022>.
- 607 Jafari, S.M., Assadpoor, E., He, Y., & Bhandari, B. (2008). Re-coalescence of droplets during  
608 high-energy emulsification. *Food Hydrocolloids*, 22, 1191-1202.  
609 <https://doi.org/10.1016/j.foodhyd.2007.09.006>
- 610 Jiang, S., Altaf Hussain, M., Cheng, J., Jiang, Z., Geng, H., Sun, Y., Sun, C., & Hou, J. (2018).  
611 Effect of heat treatment on physicochemical and emulsifying properties of polymerized  
612 whey protein concentrate and polymerized whey protein isolate. *LWT-Food Science and*  
613 *Technology*, 98, 134-140. <https://doi.org/10.1016/j.lwt.2018.08.028>.
- 614 Jones, O.G. & McClements, D.J. (2010). Biopolymer nanoparticles from heat-treated  
615 electrostatic protein-polysaccharide complexes. Factors affecting particle characteristics.  
616 *Journal of Food Science*, 72(2), N36-N43. [https://doi.org/10.1111/j.1750-](https://doi.org/10.1111/j.1750-3841.2009.01512.x)  
617 [3841.2009.01512.x](https://doi.org/10.1111/j.1750-3841.2009.01512.x).
- 618 Jones, O.G. & McClements, D.J. (2011). Recent progress in biopolymer nanoparticle and  
619 microparticle formation by heat-treating electrostatic protein-polysaccharide complexes.

- 620 *Advances in Colloid and Interface Science*, 167, 49-  
621 62. <https://doi.org/10.1016/j.cis.2010.10.006>.
- 622 Kamerzell, T.J., Esfandiary, R., Joshi, S.B., Middaugh, C.R., & Volkin, D.B. (2011). Protein-  
623 excipient interactions: Mechanisms and biophysical characterization applied to protein  
624 formulation development. *Advanced Drug Delivery Reviews*, 63, 1118-  
625 1159. <https://doi.org/10.1016/j.addr.2011.07.006>.
- 626 Laplante, S., Turgeon, S.L., & Paquin, P. (2005). Effect of pH, ionic strength, and  
627 composition on emulsion stabilizing properties of chitosan in a model system containing  
628 whey protein isolate. *Food Hydrocolloids*, 19, 721-729.  
629 <https://doi.org/10.1016/j.foodhyd.2004.08.001>.
- 630 Liu, J., Verespej, E., Alexander, M., & Corredig, M. (2007). Comparison on the effect of  
631 high-methoxyl pectin or soybean-soluble polysaccharide on the stability of sodium  
632 caseinate-stabilized oil/water Emulsions. *Journal of Agricultural and Food Chemistry*. 55,  
633 6270-6278. <https://pubs.acs.org/doi/abs/10.1021/jf063211h>
- 634 Madureira, A. R., Pereira, C. I., Gomes, A. M., Pintado, M. E., & Malcata, F. X. (2007).  
635 Bovine whey proteins-Overview of their main biological properties. *Food Research*  
636 *International*, 40, 1197-1211. <https://doi.org/10.1016/j.foodres.2007.07.005>.
- 637 Merefati, A., Rayner, M., Timgrem, A., Dejmek, P., & Sjöo, M. (2013). Freezing and freeze-  
638 drying of Pickering emulsions stabilized by starch granules. *Colloids and Surfaces A:*  
639 *Physicochemical and Engineering Aspects*, 436, 512-520.  
640 <http://dx.doi.org/10.1016/j.colsurfa.2013.07.015>.
- 641 Markwell, M.A., Hass, S.M., Bieber, L.L, & Tolbert, N.E (1978). A modification of the  
642 Lowry method to simplify the protein determination in membrane and lipoprotein samples.  
643 *Analytical Biochemistry*, 87, 206-210. [https://doi.org/10.1016/0003-2697\(78\)90586-9](https://doi.org/10.1016/0003-2697(78)90586-9)

- 644 Mitidieri, F.E., & Wagner, J.R. (2002). Coalescence of o/w emulsions stabilized by whey and  
645 isolate soybean proteins. Influence of thermal denaturation, salt addition and competitive  
646 interfacial adsorption. *Food Research International*, 35, 547-557.  
647 [https://doi.org/10.1016/S0963-9969\(01\)00155-7](https://doi.org/10.1016/S0963-9969(01)00155-7).
- 648 Monagan, F., Sherman, J. B., & Kinsella, J.E. (1995). Effect of pH and temperature on protein  
649 unfolding and thiol/disulfide interchange reactions during heat-induced gelation of whey  
650 proteins. *Journal of Agricultural and Food Chemistry*, 43, 46-52.  
651 <https://pubs.acs.org/doi/10.1021/jf00049a010>
- 652 Nakamura, A., Yoshida, R. Maeda, H., & Corredig, M. (2006). Soy soluble polysaccharide  
653 stabilization at oil-water interfaces. *Food Hydrocolloids*, 20, 277-283.  
654 <https://doi.org/10.1016/j.foodhyd.2005.02.018>.
- 655 Nakamura, A., Yoshida, R., Maeda, H., Furuta, H., & Corredig (2004). Study of the role of the  
656 carbohydrate and protein moieties of soy soluble polysaccharides in their emulsifying  
657 properties. *Journal of Agricultural and Food Chemistry*, 52, 5506-5512.  
658 <https://pubs.acs.org/doi/abs/10.1021/jf049728f>
- 659 Palazolo, G.G., Sobral, P.A., & Wagner, J.R. (2011). Freeze-thaw stability of oil-in-water  
660 emulsions prepared with native and thermally-denatured soybean isolates. *Food*  
661 *Hydrocolloids*, 25, 398-409. <https://doi.org/10.1016/j.foodhyd.2010.07.008>.
- 662 Palazolo, G.G., Sobral, P.A., & Wagner, J.R. (2016). Impact of sample aging on freeze-thaw  
663 stability of oil-in-water emulsions prepared with soy protein isolates. *International Journal*  
664 *of Food Properties*, 19, 2322-2337. <https://doi.org/10.1080/10942912.2015.1126724>.
- 665 Ray, M. & Rousseau D. (2013). Stabilization of oil-in-water emulsions using mixtures of  
666 denatured soy whey proteins and soluble soybean polysaccharides. *Food Research*  
667 *International*, 52, 298-307. <https://doi.org/10.1016/j.foodres.2013.03.008>.

- 668 Thiebaud, M., Dumay, E.M., & Cheftel, J.C. (2002). Pressure-shift freezing of o/w emulsions:  
669 influence of fructose and sodium alginate on undercooling, nucleation, freezing kinetics  
670 and ice crystal size distribution. *Food Hydrocolloids*, 16, 527-  
671 545. [https://doi.org/10.1016/S0268-005X\(01\)00133-3](https://doi.org/10.1016/S0268-005X(01)00133-3).
- 672 Wang, S., Shi, Y., Tu, Z., Zhang, L., Wang, H., Tian, M., & Zhang, N. (2017). Influence of  
673 soy lecithin concentration on the physical properties of whey protein isolate-stabilized  
674 emulsion and microcapsule formation. *Journal of Food Engineering*, 207, 73-80.  
675 <https://doi.org/10.1016/j.jfoodeng.2017.03.020>.
- 676 Xu, D., Zhang, J., Cao, Y., Wang, J., & Xiao, C. (2016). Influence of microcrystalline  
677 cellulose on the microrheological property and freeze-thaw stability of soybean protein  
678 hydrolysate stabilized curcumin emulsion. *LWT-Food Science and Technology*, 66, 590-  
679 597. <http://dx.doi.org/10.1016/j.lwt.2015.11.002>.
- 680 Xu, Y-T., & Liu, L-l (2016). Structural and functional properties of soy protein isolates  
681 modified by soluble soybean polysaccharides. *Journal of Agricultural and Food*  
682 *Chemistry*. 64, 7275-7284. <https://pubs.acs.org/doi/abs/10.1021/acs.jafc.6b02737>.
- 683 Zhu, X-F., Zhang, N., Lin, W-F., & Tang, C-H. (2017a). Freeze-thaw stability of Pickering  
684 emulsions stabilized by soy and whey protein particles. *Food Hydrocolloids*, 69, 173-184.  
685 <https://doi.org/10.1016/j.foodhyd.2017.02.001>.
- 686 Zhu, X-F., Zheng, J., Liu, F., Qiu, C-H., Lin, W-F., & Tang, C-H. (2017b). The influence of  
687 ionic strength on the characteristics of heat-induced soy protein aggregate nanoparticles  
688 and the freeze-thaw stability of the resultant Pickering emulsions. *Food & Function*, 8,  
689 2974-2981. <http://dx.doi.org/10.1039/C7FO00616K>.
- 690 Zhu, X-F., Zheng, J., Liu, F., Qiu, C-H., Lin, W-F., & Tang, C-H. (2018). Freeze-thaw  
691 stability of Pickering emulsions stabilized by soy protein nanoparticles. Influence of ionic

692 strength before or after emulsification. *Food Hydrocolloids*, 74, 37-45.

693 <https://doi.org/10.1016/j.foodhyd.2017.07.017>.

694

ACCEPTED MANUSCRIPT

**Figure captions**

**Figure 1:** Schematic representation of obtaining of aqueous dispersions prepared from whey protein isolate (WPI, 2.0% w/w), soluble soybean polysaccharides (SSPS, 0.5% w/w) and their mixtures. The assembly of complexes was performed by pH adjustment to 3.0 without or with heating. The sample nomenclature was defined according to the order of SSPS addition respect to pH adjustment and heating. The visual appearance of dispersions is also showed.

**Figure 2:** a) Turbidity profiles during acid titration (1.0 M HCl solution) of whey protein isolate (WPI), soluble soybean polysaccharides (SSPS) and WPI/SSPS mixture; b) Visual appearances of WPI, SSPS and WPI/SSPS dispersions after acid titration at pH 3.0. Biopolymer dispersions (2.0% and 0.5% w/w for WPI and SSPS, respectively) were previously diluted 1:3 v/v with distilled water before HCl addition.

**Figure 3:** a)  $\zeta$ -potential, b) non-sedimentable protein content (% w/w) and c) hydrodynamic, z-average diameters ( $D_z$ ) of unheated and heated (90 °C, 15 min) WPI (2.0%) or WPI/SSPS (2.0/0.5 % w/w) dispersions (pH 3.0). The non-sedimentable nanoparticles were obtained by centrifugation (Section 2.4, Eq. 1). The sample nomenclature was defined in Fig. 1. Values are means of three replicates ( $n=3$ ) and error bars indicate standard deviation. For  $\zeta$ -potential and non-sedimentable protein content, the mean values with different lowercase letters at the top of bars indicate significant difference ( $p < 0.05$ ). For  $D_z$  values, the mean values ( $n=3$ ) with different lowercase letters at the top of bars, indicate significant differences between different samples ( $p < 0.05$ ). The mean values with different uppercase letters indicate significant differences between  $D_z$  values in the total and non-sedimentable fraction ( $p < 0.05$ ).

**Figure 4:** a) Aromatic surface hydrophobicity values ( $H_0$ ) and b) Effect of various perturbing agents on the turbidity of aqueous dispersions (pH 3.0) prepared with WPI (2.0% w/w) or WPI/SSPS (2.0/0.5% w/w). For turbidity assays, the dispersions were diluted (1:3 v/v) with distilled water, urea 6.0 M solution or urea 6.0 M/dithiothreitol (DTT) 30 mM solution. The sample nomenclature



was defined in Fig. 1. Values are means of three replicates ( $n=3$ ) and error bars indicate standard deviation. For  $H_0$ , the mean values with different lowercase letters at the top of bars indicate significant differences ( $p < 0.05$ ). For turbidity, the mean values with different lowercase letters at the top of bars, indicate significant differences between different samples ( $p < 0.05$ ). The mean values with different uppercase letters indicate significant differences between turbidity values measured with different perturbing agents ( $p < 0.05$ ).

**Figure 5:** Evolvement of interfacial complex viscosity ( $\eta^*$ ) at the oil/water interface against time for the total (a, b) and non-sedimentable fraction (c) of unheated and heated WPI (2.0% w/w) or WPI/SSPS dispersions (pH 3.0). The non-sedimentable nanoparticles were obtained by centrifugation (Section 2.4, Eq. 1). The sample nomenclature was defined in Fig. 1.

**Figure 6:** De Brouckere volume-weighted mean diameter ( $D_{4,3}$ ) and 90<sup>th</sup> volume percentile ( $D_{v,0.9}$ ) of initial and freeze-thawed emulsions ( $-18 \pm 2$  °C) prepared with different aqueous dispersions (pH 3.0) of WPI (2.0% w/w) and WPI/SSPS mixtures (2.0/0.5% w/w). Both parameters were obtained from particle size distributions measured in the presence 1.0% w/v SDS solution at pH 3.0. The sample nomenclature was defined in Fig.1. Values are means of three replicates ( $n=3$ ) and error bars indicate standard deviation. The mean values with different lowercase letters at the top of bars indicate significant differences ( $p < 0.05$ ) between different emulsions. The mean values with different uppercase letters indicate significant differences between  $D_{4,3}$  and  $D_{v,0.9}$  values before and after freeze-thawing.

**Table 1.** Interfacial pressure ( $\pi_i$ ) values at the oil/water interface for dispersions prepared with mixtures of whey protein isolates (WPI) and soluble soybean polysaccharides (SSPS). The sample nomenclature was defined in Fig 1.

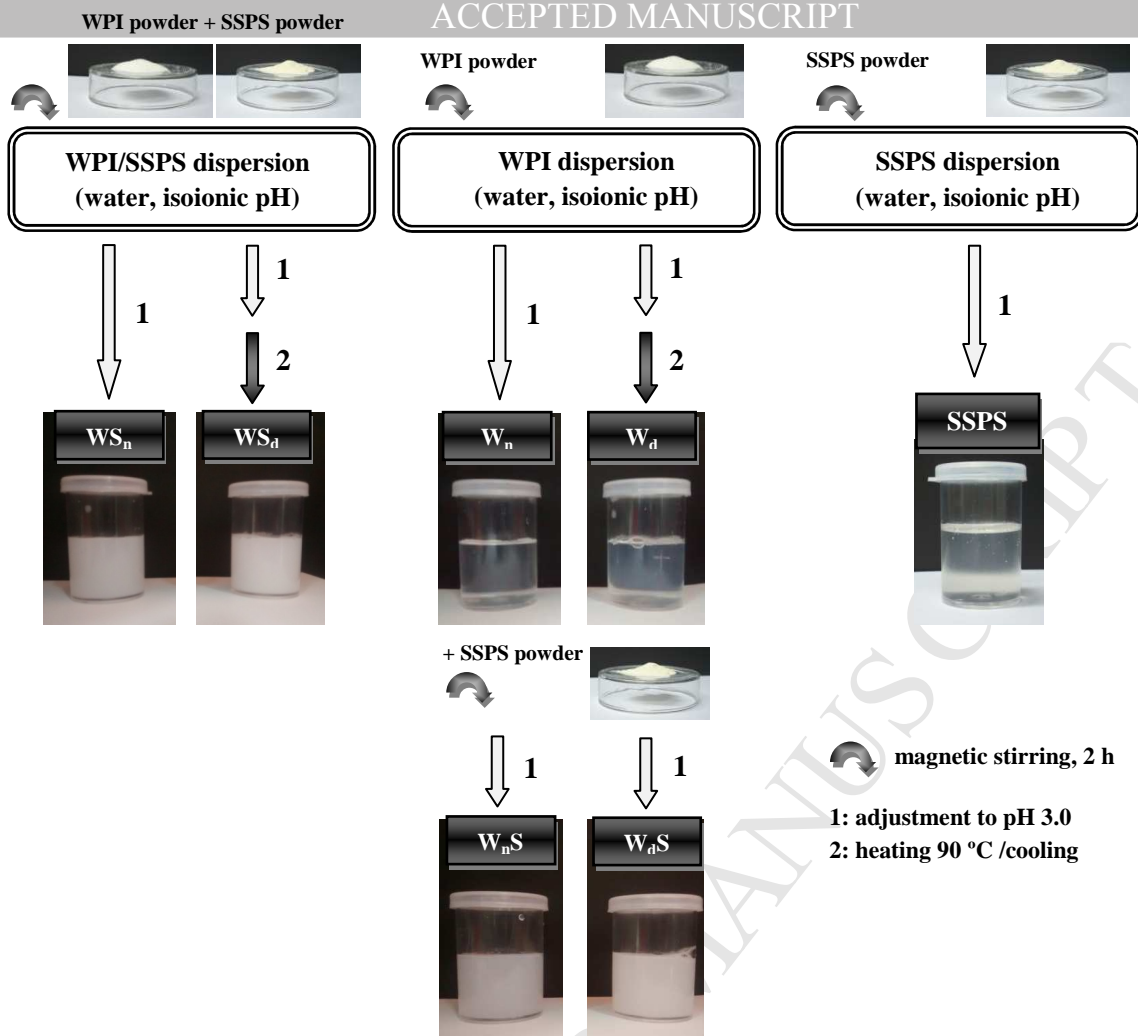
Aqueous dispersions	$\pi_i$ (mN/m)
$W_n$	$11.58 \pm 0.06^c$
$WS_n$	$12.39 \pm 0.06^a$
$W_nS$	$12.27 \pm 0.07^a$
$W_d$	$10.88 \pm 0.10^d$
$WS_d$	$11.76 \pm 0.09^b$
$W_dS$	$11.84 \pm 0.08^b$

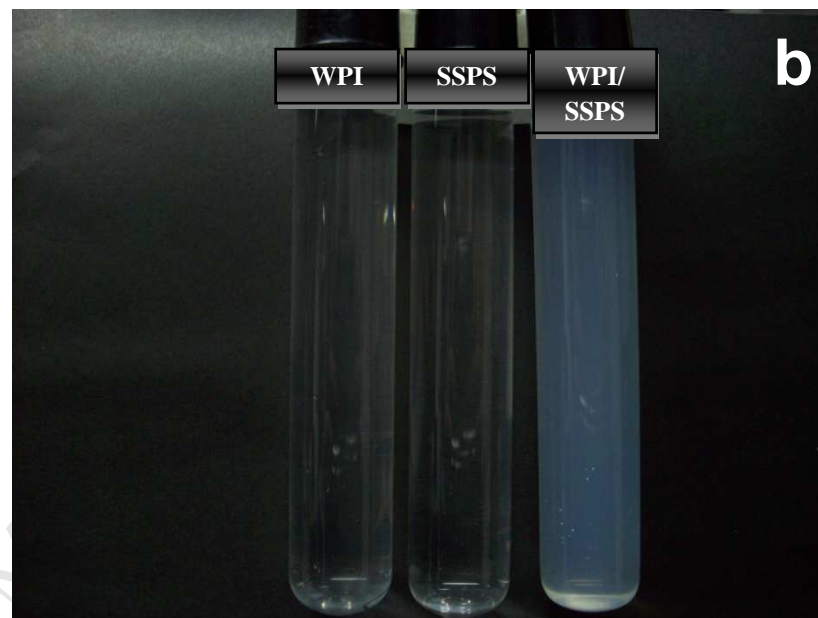
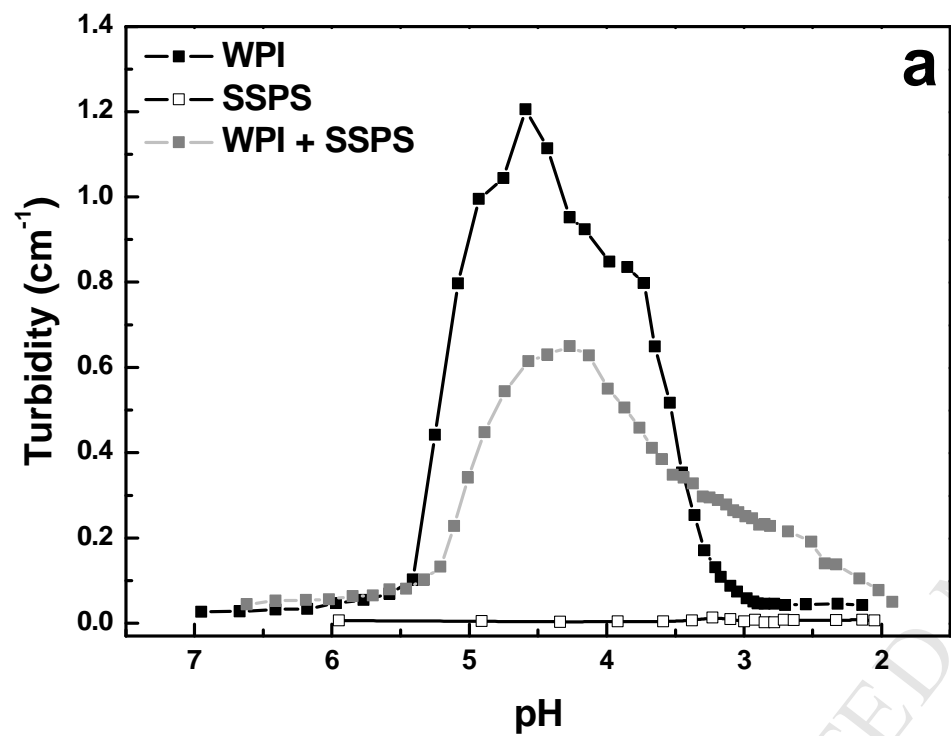
Mean values ( $n=3$ ) with different lowercase letters indicate significant differences between different aqueous dispersions, as determined by Fisher's test ( $p<0.05$ )

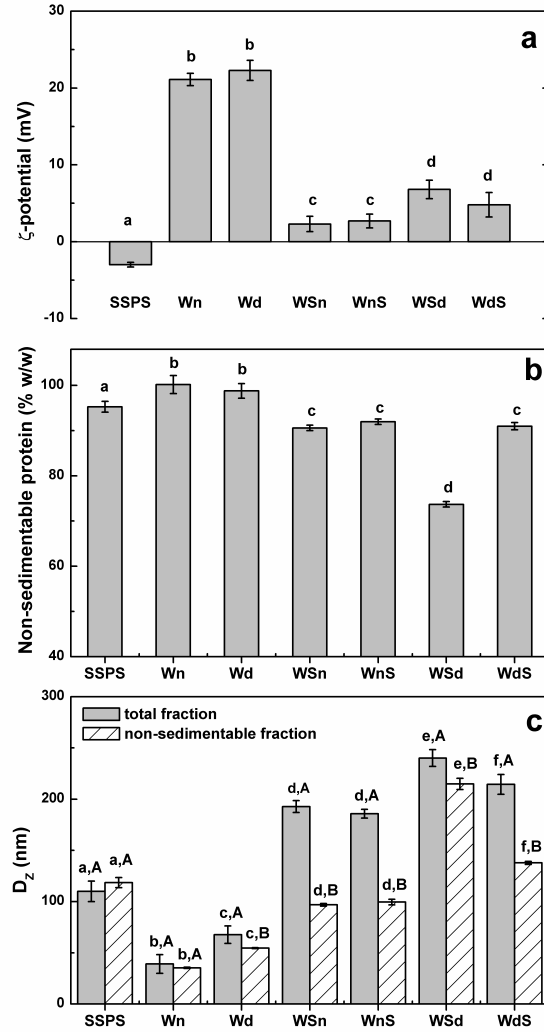
**Table 2:** Destabilization parameters (flocculation and coalescence indices, FI and CI, respectively) of initial and freeze-thawed o/w emulsions prepared with different aqueous dispersions of WPI (2.0% w/w) and WPI/SSPS mixtures (2.0/0.5% w/w). Sample nomenclature was defined in Fig.1.

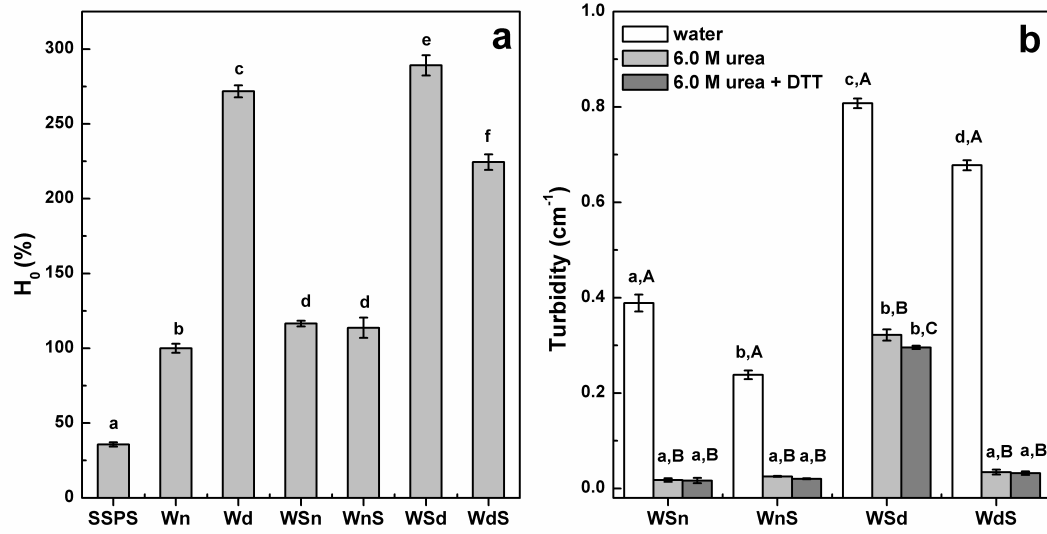
Emulsions	FI (%)		CI (%)
	Initial	After freeze-thawing	After freeze-thawing
$W_n$	$0.8 \pm 0.1^b$	$36.2 \pm 4.0^c$	$34.9 \pm 3.9^c$
$WS_n$	$2.5 \pm 0.1^a$	$19.3 \pm 2.0^d$	$13.5 \pm 1.9^d$
$W_nS$	$0.5 \pm 0.1^b$	$7.1 \pm 0.9^e$	$16.2 \pm 2.0^d$
$W_d$	$2.2 \pm 0.2^a$	$51.0 \pm 3.7^b$	$51.4 \pm 6.0^b$
$WS_d$	$0.7 \pm 0.1^b$	$154.2 \pm 5.0^a$	$107.6 \pm 3.5^a$
$W_dS$	$0.7 \pm 0.1^b$	$15.2 \pm 0.8^d$	$16.8 \pm 0.3^d$

Mean values ( $n=3$ ) with different lowercase letters within the same column indicate significant differences between different aqueous dispersions, as determined by Fisher's test ( $p<0.05$ ).

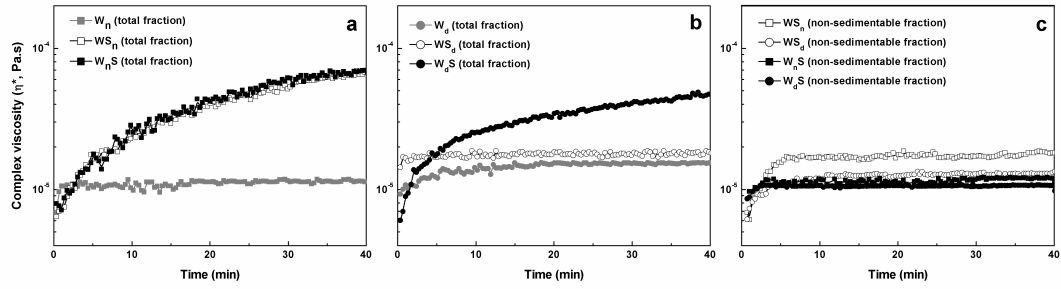






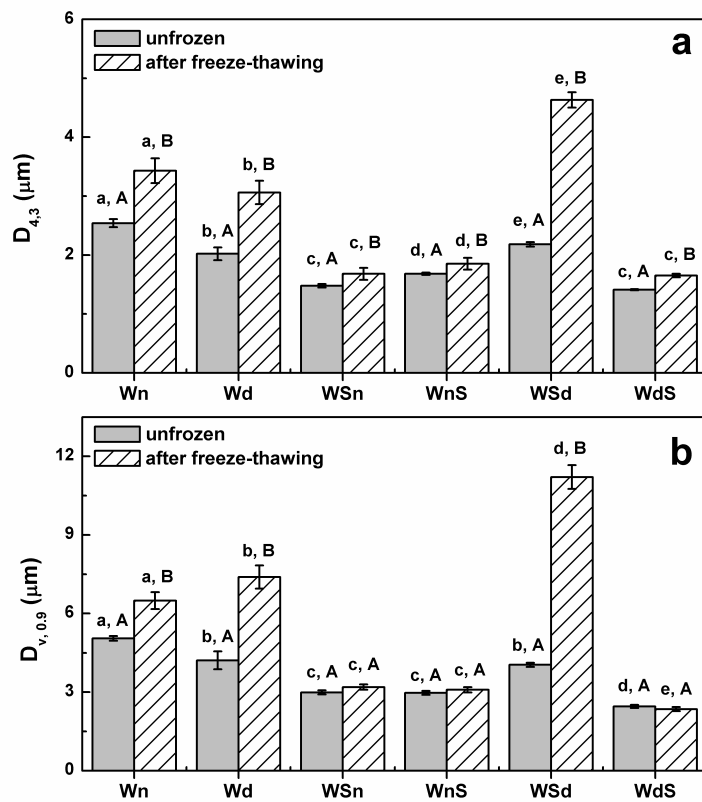


ACCEPTED



ACCEPTED TEL





**HIGHLIGHTS**

WPI/SSPS nanoparticles were assembled at pH 3.0 using different strategies.

The structural and interfacial properties of complexes depended on their assembly procedure.

Freeze-thawing was evaluated on emulsions prepared with WPI/SSPS complexes.

The freeze-thaw stability of emulsions was affected by the assembly procedure of complexes.

ACCEPTED MANUSCRIPT